Theoretical study of $[Hg_3(o\text{-}C_6F_4)_3]_n \cdot \{benzene\}$ (n = 1, 2) complexes

Fernando Mendizabal [a,*], Darwin Burgos [a], Claudio Olea-Azar [b]

[a] Departamento de Química, Facultad de Ciencias, Universidad de Chile, Casilla 653, Santiago, Chile
[b] Departamento de Química Inorgánica y Analítica, Facultad de Ciencias Químicas y Farmacéuticas, Universidad de Chile, Casilla 233, Santiago 1, Chile

A B S T R A C T

The electronic structure and spectroscopic properties of $[Hg_3(o\text{-}C_6F_4)_3]_n \cdot \{benzene\}$ (n = 1, 2) were studied at the HF, MP2 and PBE levels. The interaction between $[Hg_3(o\text{-}C_6F_4)_3]$ and benzene at the HF and MP2 levels was analyzed. Secondary π-interactions (Hg–benzene) were found to be the main contribution short-range stability in the $[Hg_3(o\text{-}C_6F_4)_3] \cdot \{benzene\}$ complex. At the MP2 and PBE levels equilibrium Hg–C distances of 338.4 and 361.4 pm; and interaction energies of 46.6 and 29.2 kJ/mol were found, respectively. The absorption spectra of these complexes were calculated by the single excitation time-dependent method at PBE level.

1. Introduction

The supramolecular chemistry of trimeric perfluoro-*ortho*-phenylenemercury $[Hg_3(o\text{-}C_6F_4)_3]$ forming adducts with a variety of arenes (benzene, biphenyl, naphthalene, etc.), aldehydes, ketones, amides, nitriles, phosphoramides, and sulfoxides has been widely investigated, mostly by Gabbaï and co-workers [1–7].

This class of compounds have been reported to form adducts with interesting coordination chemistry. In general, the donor–acceptor interaction invokes dispersion and electrostatic intermolecular forces that probably add to the stability to the adducts [8,9].

Theoretical DFT studies of the $[Hg_3(o\text{-}C_6F_4)_3]$ complex indicate that the LUMO spans the three mercury centers (6p) and forms a large lobe that protrudes above and below the molecular plane [9]. The result suggests that this particular region of the molecule is where Lewis acidity (acceptor) is at a maximum. In agreement with that, this large lobe appears directly aligned with the direction along which Lewis base substrates approach the molecule [9].

We are interested in the $[Hg_3(o\text{-}C_6F_4)_3] \cdot \{benzene\}$ adduct. The structural results show the formation of extended stacks that consist of nearly parallel complexes, with staggered molecules of $[Hg_3(o\text{-}C_6F_4)_3]$ complex that sandwich benzene molecules [1]. In the adduct formed, secondary π-interactions are suggested between the mercury atoms and the benzene molecule. The Hg–C(benzene) distances are between 341 and 346 pm [1,3]. The orientation between $[Hg_3(o\text{-}C_6F_4)_3]$–benzene is almost planar. NMR spectroscopy results indicate that the benzene molecule undergoes an in-plane 60° reorientation with an activation energy of 52 ± 4 kJ/mol [3]. The magnitude of this activation energy suggests the presence of directional interactions between the mercury atoms and the benzene molecule.

Others aromatic substrates (arene: biphenyl, naphthalene, pyrene, etc.) form binary adducts with $[Hg_3(o\text{-}C_6F_4)_3]$ analogous to those with benzene [2,3]. The Hg–C(arene) distances are in the range 325 and 355 pm. The contacts possibly reflect the presence of secondary polyhapto-π interactions. Also, these adducts display an intense room temperature photoluminescence in the UV–visible spectrum.

When there are two or more very heavy atoms (gold, thallium, mercury, etc.) in the complexes studied, they show evidence of metallophilic interactions. At theoretical level, the metallophilic attraction is estimated when electronic correlation effects are taken into account, strengthened by relativistic effects [10,11]. Closed-shell metallophilic interactions (d^{10}–d^{10}, d^8–d^8, s^2–s^2, etc.) are estimated to be energetically similar to hydrogen bonds (20–50 kJ/mol) [11]. The mechanism behind such attraction is the dispersion (van der Waals) interaction, with additional allowance for virtual charge-transfer terms [11]. Moreover, we have studied theoretically the attraction between small ligands (C_2H_2, C_2H_4 and CO) and metal (Au, Tl^+) using ab initio methodology (MP2 to CCSD(T)) [12–14]. In all the complexes, dispersion interaction is the principal contribution to stability.

The optical properties of molecules can be calculated from CIS and higher levels [15,16]. However, the predicted power of density functional theory (DFT) with the time-dependent (DFT-TD) approach makes it the method of choice. Several reports have shown an excellent association with experimental absorption and emission spectra in different systems [17–20].

The aim of the present work is to study the $[Hg_3(o\text{-}C_6F_4)_3]_n \cdot \{benzene\}$ (n = 1, 2) complexes at a theoretical level and relate them to their excitation spectra. We propose to study the effect of several complexes and how their interactions can influence the spectroscopic absorption properties. To our knowledge, so far no systematic TD-DFT investigations have been made on these systems.

* Corresponding author. Fax: +(562) 271 3888.
E-mail address: hagua@uchile.cl (F. Mendizabal).

2. Models and methods

The models $[Hg_3(o\text{-}C_6F_4)_3]_n \cdot \{benzene\}$ ($n = 1, 2$) used in our study are depicted in Fig. 1. The geometries were fully optimized at the scalar relativistic HF, MP2 ($n = 1$) and PBE ($n = 1, 2$) (Perdew–Burke–Ernzerhof) [21] levels in the gas phase. The MP2 calculation implies a large computational effort and was only used for model **1**. Single point calculations of these geometries were simulated to study the excitation spectra with TD-DFT by PBE. Regarding this method, PBE has been used in the study of weak interactions [22,23]. It is the best available functional for dispersion forces, without parameters fitted to experimental data. However, none of the existing functionals are optimal for evaluating the dispersion interaction [24].

The excitation energies were obtained at the PBE level by using the time-dependent perturbation theory approach (TD-DFT) [25,26], which is based on the random-phase approximation (RPA) method [27]. The TD-DFT calculations do not evaluate the spin–orbit splitting, and the values are averaged.

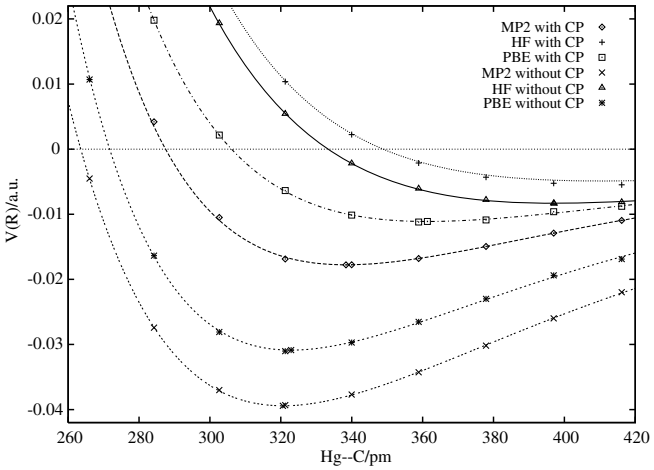

Fig. 2. Interaction potential between Hg and benzene in $[Hg_3(o\text{-}C_6F_4)_3] \cdot \{benzene\}$ (**1**) at the HF and MP2 levels.

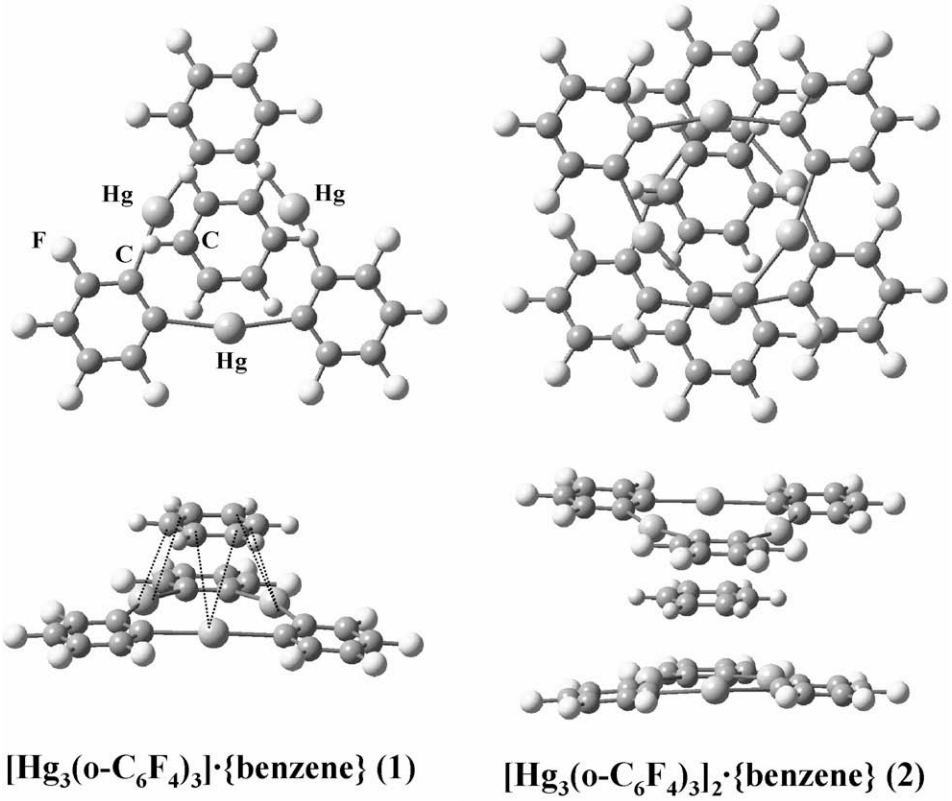

Fig. 1. $[Hg_3(o\text{-}C_6F_4)_3]_n \cdot \{benzene\}$ ($n = 1, 2$) models (**1**, **2**).

Table 1
Main geometric parameters of the $[Hg_3(o\text{-}C_6F_4)_3]_n \cdot \{benzene\}$ ($n = 1, 2$) systems (distances in pm and angles in degrees)

System	Method	Hg–Hg[a]	HgC[b]	HgC[c]	CC	CF	HgCC (°)	HgHgHg (°)
$[[Hg_3(C_6F_4)_3] \cdot \{benzene\}$ (**1**) (C_1)	HF	461.7	242.5	383.2	138	131	131.3	60.2
	MP2	401.9	234.2	318.8	133	133	124.1	59.3
	PBE	431.5	238.7	330.3	133	132	127.4	59.8
$[[Hg_3(C_6F_4)_3]_2 \cdot \{benzene\}$ (**2**) (C_1)	PBE	439.5	238.8	334.8	139	134	128.5	59.6
$[[Hg_3(C_6F_5)_3]_\infty \cdot \{benzene\}$	Exp.	398.7	215.0	344.3	139	135	125.0	60.1

[a] Hg–Hg intramolecular distance.
[b] Hg–C distance $-C_6F_4$ groups.
[c] Hg–C distance C_6H_6.

Table 2
Intermolecular distance Hg–C (pm) and interaction energies, $V(R_e)$, in kJ/mol by $[Hg_3(o\text{-}C_6F_4)_3]_n \cdot$ {benzene} system with and without counterpoise (CP) correction

System	Method	Hg–C	$V(R_e)$
$[[Hg_3(C_6F_4)_3] \cdot$ {benzene} (**1**)	HF[a]	410.6	−12.8
	MP2[a]	338.4	−46.6
	PBE[a]	361.4	−29.2
$[[Hg_3(C_6F_4)_3] \cdot$ {benzene} (**1**)	HF[b]	397.1	−21.9
	MP2[b]	320.6	−103.5
	PBE[b]	322.9	−81.0

[a] With CP.
[b] Without CP.

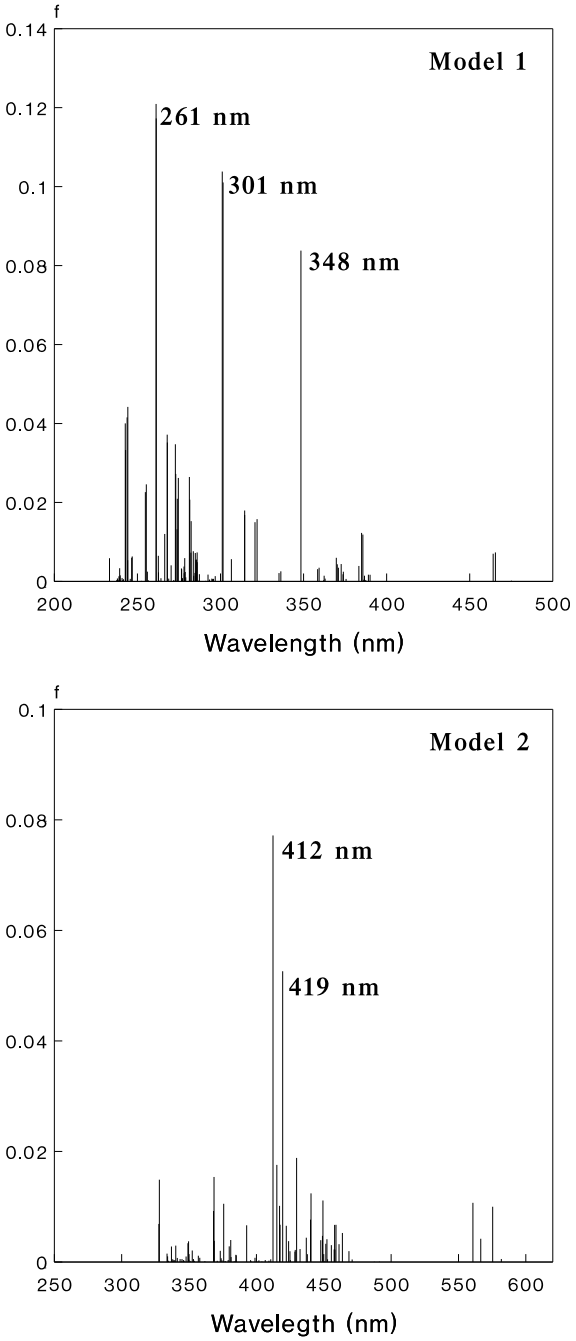

Fig. 3. Calculated electronic PBE spectra for the models (**1**, **2**).

The calculations were done using the TURBOMOLE package (version 5.9) [28]. For Hg, the 20 valence-electron (VE) quasi-relativistic (QR) pseudo-potential (PP) of Andrae et al. [29] was employed. We used two *f*-type polarization functions on mercury (α_f = 0.50, 1.50) [30]. Also, the C and F atoms were treated through PPs, using double-zeta basis sets with the addition of one d-type polarization function [31]. For the H atom, a double-zeta basis set plus one p-type polarization function was used [32]. For MP2 and PBE, the efficient resolution of identity (RI) approximation was employed to obtain the final geometry and make the calculation feasible [33].

3. Results and discussion

3.1. Molecular geometry and secondary Hg–benzene energy

We have fully optimized the geometries for the models $[Hg_3(o\text{-}C_6F_4)_3]_n \cdot$ {benzene} (n = 1, 2) (**1, 2**). Table 1 shows the main parameters, together with relevant experimental structural data. The theoretical results are in agreement with the experimental data when the $[Hg_3(o\text{-}C_6F_4)_3] \cdot$ {benzene} complex is compared at the HF, MP2 and PBE levels. It is seen that the structural parameters change from the HF and PBE to the MP2 level in model **1**. The usual correlation-induced shortening is found for MP2 calculation, suggesting intramolecular metallophilic attractions among mercury atoms. Also, the Hg–C(benzene) distances show a secondary attraction at 318.8 pm, which is shorter than the experimental value (344.3 pm). It is worth noting that the MP2 approximation overestimates the van der Waals interactions (dispersion) [11]. On the other hand, HF does not describe properly the metallophilic and metallic–carbon attraction, which is manifested in very long Hg–Hg and Hg–C distances: 461.7 and 383.2 pm, respectively.

Using the PBE method, we find an intermediate situation. The closest Hg–Hg distances in the **1** and **2** models are: 431.5 and 439.5 pm. The Hg–C(benzene) distances are 330.3 and 334.8 pm, very close to the experimental value (344.3 pm). The latter results should be analyzed with caution, since DFT calculations do not describe appropriately the van der Waals (dispersion) attractions; though DFT can occasionally reproduce the van der Waals distance [24].

Table 3
TD-DFT/PBE singlet-excitation calculations for $[Hg_3(o\text{-}C_6F_4)_3]_n \cdot$ {benzene} (n = 1, 2)

System	λ_{calc} (nm)	f[a]	λ_{exp} (nm)	Contributions[b]	Transition type
$[Hg_3(C_6F_4)_3] \cdot$ {benzene}	261	0.1209		113a → 124a (26)	MLMCT (s + pσ → s + d)
				123a → 139a (8)	MLMCT (pσ → s*)
	301	0.1038		116a → 127a (39)	LMCT (π* → s + p)
				117a → 127a (22)	LMCT (π* → s + p)
				118a → 127a (18)	LMCT (π* → s + p)
	348	0.0838		117a → 126a (32)	LMCT (π* → s + dz^2)
				116a → 125a (31)	LMCT (π* → dz^2)
				119a → 126a (11)	LMCT (π* → s + dz^2)
$[Hg_3(C_6F_4)_3]_2 \cdot$ {benzene}	412	0.0771		214a → 233a (35)	LMCT (π* → s + dz^2)
				215a → 233a (33)	MLMCT (s + pσ → s + dz^2)
	419	0.0526		218a → 233a (31)	LMCT (π* → s + dz^2)
				215a → 232a (21)	MLMCT (s + pσ → s + dz^2)

[a] Oscillator strength.
[b] Values are |coeff.|^2 × 100.

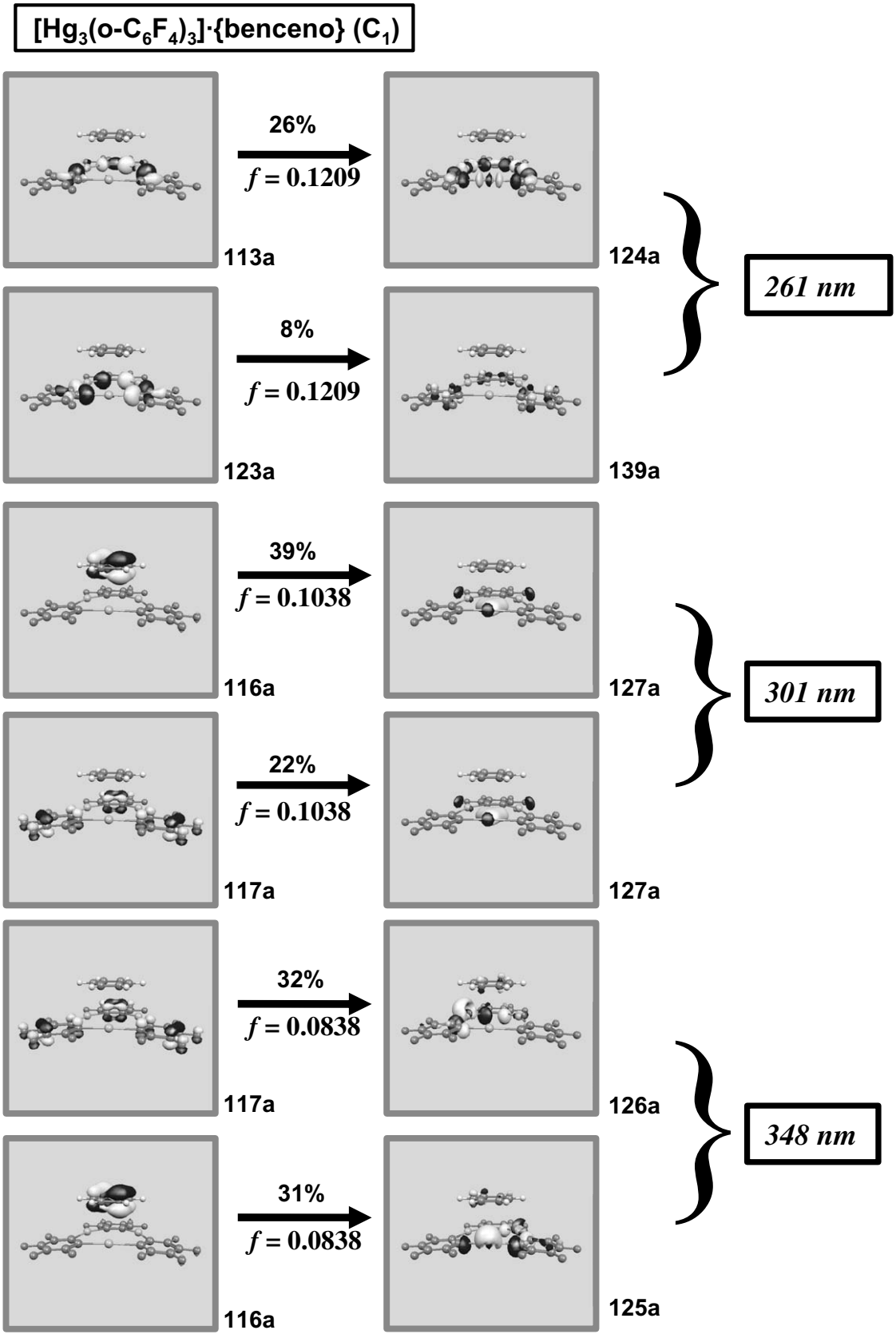

Fig. 4. Active molecular orbitals in the electronic transitions of $[Hg_3(o\text{-}C_6F_4)_3] \cdot \{benzene\}$ (**1**) at the PBE level.

We have estimated the intermolecular interaction $[Hg_3(o\text{-}C_6F_4)_3]$–benzene energies for model **1** with and without counterpoise correction (CP) for the basis-set superposition error (BSSE). The results are shown in Fig. 2 and Table 2. The model with CP

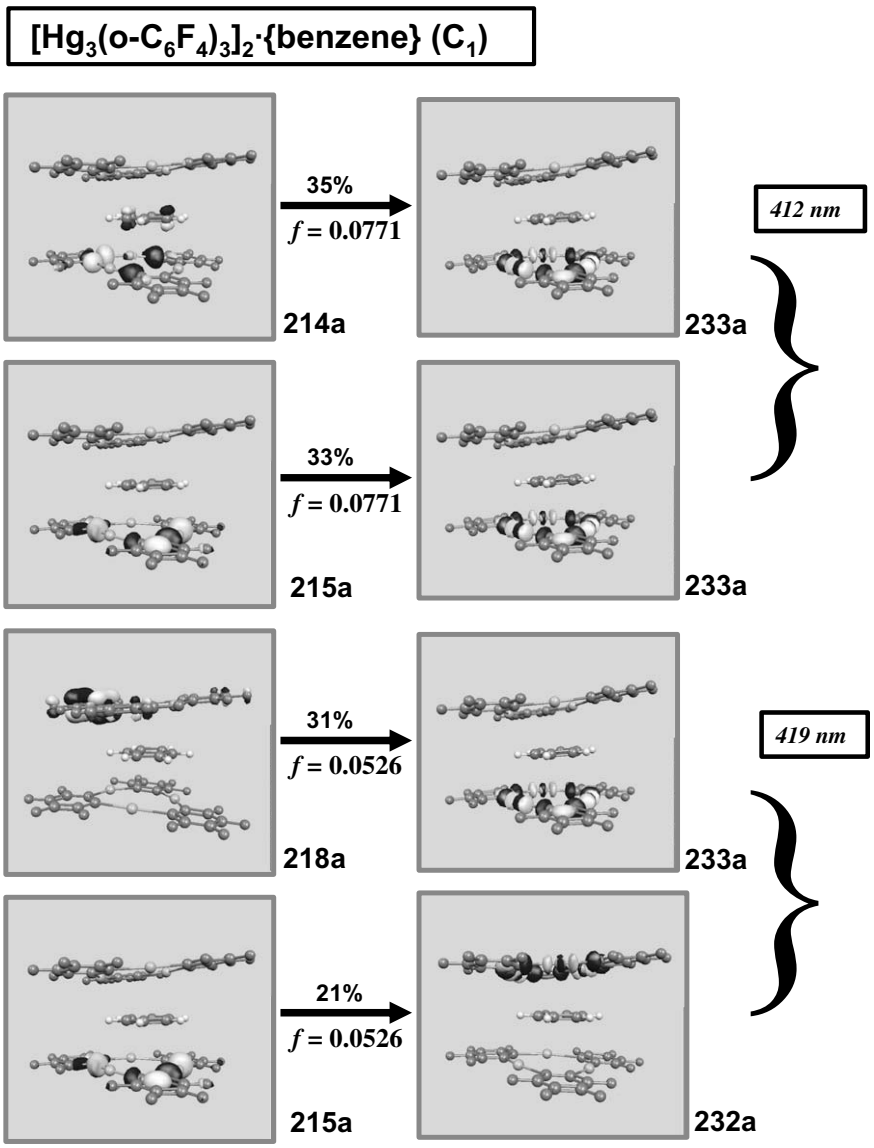

Fig. 5. Active molecular orbitals in the electronic transitions of $[Hg_3(o\text{-}C_6F_4)_3]_2 \cdot \{benzene\}$ (**2**) at the PBE level.

produces an attraction at the MP2 and PBE levels. We obtain a shorter equilibrium Hg–C(benzene) distance of 338.4 and 361.4 pm with an interaction energy of 46.6 and 29.2 kJ/mol, respectively. At the HF level there is no evident minimum. The electrostatic and induction contributions would still be there. One may expect that the inclusion of *f* functions on mercury atoms should reduce the BSSE. However, as it is appreciated in Fig. 2 and Table 2, the interaction energies without CP are strongly overestimated at all levels. These results replicate the distances reported in optimizing geometry: 320.6 and 322.9 pm at the MP2 and PBE levels, respectively.

We associate the secondary Hg–benzene interaction as the MP2 and PBE energies at the equilibrium distance of 338.4 and 361.4 pm, respectively. If the interaction energy, $V(R_e)$, is divided by the number of closest Hg–C(beneze) contacts present in the model, pair-wise energies of 7.8 and 4.9 kJ/mol are found at the MP2 and PBE levels, a value that is in the theoretical range. We have found that the energy interaction is mainly due to an electronic correlation effect. The difference between the two methods is due in the treatment of the electronic correlation. From a theoretical point of view, in literature is reported the model $[AuPh_2][Ag_4(CO_2H)_5]^{2-}$, where it has been estimated interaction $Ag–C_{ipso}$ of a phenyl ring in 21.5 kJ/mol at the MP2 level [34].

3.2. Time-dependent (TD) DFT calculations

For this adduct, the UV–visible spectra has not been reported experimentally. We have evidence that other arenes (biphenyl, naphthalene, pyrene, etc.) display an intense room temperature photoluminescence in the UV–visible spectrum [2,3]. For that reason, we propose theoretical spectra for models **1** and **2**.

We calculated the allowed spin singlet transition for this complex, based on the ground state structures of models **1** and **2** at the PBE level. Only singlet–singlet transitions were considered in these scalar relativistic calculations. Here, we consider as permitted transitions those whose oscillator strength is different of zero. The allowed transitions obtained are shown in Fig. 3 and Table 3. The active molecular orbitals in electronic transitions at the PBE level are shown in Figs. 4 and 5.

3.2.1. $[Hg_3(o\text{-}C_6F_4)_3] \cdot \{benzene\}$ (**1**)

The electronic structure of the model has been described with three absorption peaks at 261, 301 and 348 nm assigned to

individual states of a metal–ligand-to-metal and ligand-to-metal charge transfer (MLMCT and LMCT). The theoretical calculations are described in Table 2.

The bands are a mixture of excitations. The transition at 261 nm is composed mainly of 113a ($s + p\sigma$) → 124a ($s + d$) and 123a ($p\sigma$) → 139a (s^*). This band corresponds to MLMCT. The second transition at 301 nm has two principal excitations 116a (π^*) → 127a ($s + p$) and 117a (π^*) → 127a ($s + p$), which is associated with LMCT. The third transition at 348 nm shows two principal component 117a (π^*) → 126a ($s + dz^2$) and 116a (π^*) → 125a (dz^2) of the LMCT type. We must point out that the 116a orbital corresponds to a π^* orbital of the benzene molecule. Thus, the transition involved this orbital goes to a mercury complex orbital. The active molecular orbitals in the electronic transition are shown in Fig. 4.

*3.2.2. $[Hg_3(o\text{-}C_6F_4)_3]_2 \cdot \{benzene\}$ (**2**)*

When we used model **2**, we observed a red shift of the excited bands at 412 and 419 nm (see Table 2). The bands are mainly a double LMCT and MLMCT of type $\pi^* \rightarrow s + dz^2$ and $s + p\sigma \rightarrow s + dz^2$, which can be understood from the M.Os shown in Fig. 5. A shift in the wavelength of the excitation bands is observed by addition of a second mercury complex. The 214a → 233a transition involves the benzene-to-mercury complex orbital.

4. Conclusion

This study provides further information on the nature of the mercury–carbon(benzene) intermolecular interaction in the $[Hg_3(o\text{-}C_6F_4)_3]_n \cdot \{benzene\}$ ($n = 1, 2$) complexes and on their spectroscopic properties. Theoretical calculations at the MP2 and PBE levels are in agreement with experimental geometries and secondary π-interactions. We have found that the energy interaction is mainly due to an electronic correlation effect. Moreover, the interaction energies without BSSE are strongly overestimated. On the other hand, the aim of TD-DFT/PBE calculations was to predict the excitation spectra. The results show a mixture of type MLMCT and LMCT excitations in model **1**, with participation of the benzene molecule. Model **2** retained the transition contribution described for model **1**. A red shift effect is seen when a second mercury complex is included.

Acknowledgement

This research was financed by FONDECYT under Project 1060044 (Conicyt-Chile).

References

[1] M. Tsunoda, F.P. Gabba, J. Am. Chem. Soc. 122 (2000) 8335.
[2] M.R. Haneline, M. Tsunoda, F.P. Gabba, J. Am. Chem. Soc. 124 (2002) 3737.
[3] M.R. Haneline, R.E. Taylor, F.P. Gabba, Chem. Eur. J. 9 (2003) 5189.
[4] M.R. Haneline, J.B. King, F.P. Gabba, Dalton Trans. (2003) 2686.
[5] C. Burress, O. Elbjeirami, M.A. Omary, F.P. Gabba, J. Am. Chem. Soc. 127 (2005) 12166.
[6] T.J. Taylor, F.P. Gabba, Organometallics 25 (2006) 2143.
[7] T.J. Taylor, C.N. Burress, F.P. Gabba, Organometallics 26 (2007) 5252.
[8] A. Burini et al., J. Am. Chem. Soc. 122 (2000) 11264.
[9] M.R. Haneline, F.P. Gabba, Inorg. Chem. 44 (2005) 6248.
[10] P. Pyykkö, Angew. Chem. Int. Ed. Engl. 43 (2004) 4412.
[11] P. Pyykkö, F. Mendizabal, Inorg. Chem. 37 (1998) 3018.
[12] F. Mendizabal, Int. J. Quantum Chem. 73 (1999) 317.
[13] F. Mendizabal, Organometallics 20 (2001) 261.
[14] F. Mendizabal, C. Olea-Azar, Int. J. Quantum Chem. 107 (2007) 232.
[15] H.-X. Zhang, C.-M. Che, Chem. Eur. J. 7 (2001) 4887.
[16] Q.-J. Pan, H.-X. Zhang, Eur. J. Inorg. Chem. (2003) 4202.
[17] E.J. Fernández, M.C. Gimeno, A. Laguna, J.M. López-deLuzuriaga, M. Monge, P. Pyykkö, D. Sundholm, J. Am. Chem. Soc. 122 (2000) 7287.
[18] E.J. Fernández, P.G. Jones, A. Laguna, J.M. López-de-Luzuriaga, M. Monge, J. Pérez, M.E. Olmos, Inorg. Chem. 41 (2002) 1056.
[19] F. Mendizabal, C. Olea-Azar, Int. J. Quantum Chem. 103 (2005) 34.
[20] F. Mendizabal, B. Aguilera, C. Olea-Azar, Chem. Phys. Lett. 447 (2007) 345.
[21] J.P. Perdew, K. Burke, M. Ernzerhof, Phys. Rev. Lett. 77 (1996) 3865.
[22] Y.-B. Wang, Z. Lin, J. Am. Chem. Soc. 125 (2003) 6072.
[23] E.R. Johnson, G.A. DiLabio, Chem. Phys. Lett. 419 (2006) 333.
[24] M.P. Johansson, D. Sundholm, J. Vaara, Angew. Chem. Int. Ed. Engl. 43 (2004) 2678.
[25] R. Bauernschmitt, R. Ahlrichs, Chem. Phys. Lett. 256 (1996) 454.
[26] M.E. Casida, C. Jamorski, K.C. Casida, D.R. Salahub, J. Chem. Phys. 108 (1998) 4439.
[27] L. Olsen, P. Jorgensen, in: D.R. Yarkony (Ed.), Modern Electronic Structure Theory, vol. 2, World Scientific, River Edge, NJ, 1995.
[28] R. Ahlrichs, M. Bär, M. Häser, H. Horn, C. Kölmel, Chem. Phys. Lett. 162 (1989) 165.
[29] D. Andrae, U. Häusserman, M. Dolg, H. Stoll, H. Preuss, Theor. Chim. Acta 77 (1990) 123.
[30] P. Pyykkö, M. Straka, T. Tamm, Phys. Chem. Chem. Phys. 1 (1999) 3441.
[31] A. Bergner, M. Dolg, W. Küchle, H. Stoll, H. Preuss, Mol. Phys. 80 (1993) 1431.
[32] S. Huzinaga, J. Chem. Phys. 42 (1965) 1293.
[33] K. Eichkorn, O. Treutler, H. Öhm, M. Häser, R. Ahlrichs, Chem. Phys. Lett. 240 (1995) 283.
[34] E.J. Fernández, A. Laguna, J.M. López-de-Luzuriaga, M. Monge, M.E. Olmos, R.C. Puelles, J. Phys. Chem. B 109 (2005) 20652.